Journal of
Composites Science

MDPI

Article

Fabrication of h-MoO_3 Nanorods and the Properties of the MoO_3/WEP Composite Coatings Research

Ying Zhou [1,*], Cuihuan Song [1], Zhixiang Chen [1] and Qixin Zhou [2,*]

[1] Department of Materials Chemistry, Huzhou University, Huzhou 313000, China; 2017363333@stu.zjhu.edu.cn (C.S.); 2018363504@stu.zjhu.edu.cn (Z.C.)
[2] Department of Chemical, Biomolecular, and Corrosion Engineering, The University of Akron, 264 Wolf Ledges Parkway, Akron, OH 44325, USA
* Correspondence: 02662@zjhu.edu.cn (Y.Z.); qzhou@uakron.edu (Q.Z.)

Abstract: In this study, we prepared a novel coating composed of hexagonal molybdenum oxide (h-MoO_3) nanofiller and waterborne epoxy resin (WEP) to provide corrosion protection. We optimized the h-MoO_3 nanorod synthesis methodology first by changing different parameters (pH, temperature, etc.). Furthermore, the as-prepared h-MoO_3 rods were characterized using a scanning electron microscope (SEM) and X-ray diffraction (XRD). Finally, the electrochemical impedance spectroscopy (EIS) test results verified that the anticorrosive performance of the composite coatings was improved by incorporation of low content of MoO_3 nanofiller (0.5 wt.%) compared to pure WEP sample. This developed composite will provide a new insight for the design and fabrication of one-dimensional (1D) nanomaterial (e.g., nanorod) reinforced epoxy coating and other polymeric coating processes.

Keywords: waterborne epoxy; molybdenum trioxide nanorod; composites

Citation: Zhou, Y.; Song, C.; Chen, Z.; Zhou, Q. Fabrication of h-MoO_3 Nanorods and the Properties of the MoO_3/WEP Composite Coatings Research. *J. Compos. Sci.* **2021**, *5*, 207. https://doi.org/10.3390/jcs5080207

Academic Editor: Huirong Le

Received: 30 June 2021
Accepted: 2 August 2021
Published: 4 August 2021

1. Introduction

The economy is significantly impacted by corrosion in various industries. According to the World Corrosion Organization, the cost of corrosion annually in 2010 was over USD 2 trillion, which is more than 3% of global domestic product [1]. Therefore, novel anticorrosion materials are developed continuously to save total domestic costs. Epoxy resin is typically used to protect the surface of the materials since it has excellent adhesion, high mechanical strength, chemical stability, low shrinkage, etc. [2–5]. However, the pure epoxy coating has weak anticorrosion capability due to the inherent cross-linked structure, brittleness, and micropores easily forming during the solvent evaporation process, resulting in it not being able to meet the requirements in practical industry applications [6–8]. In recent years, researchers have been trying to develop nanofillers to improve the intrinsic properties of epoxy coating [9,10]. For example, the permeability and adhesion of the epoxy coating can be improved by adding nanometal Zn, SiO_2, etc. [11,12]. In this context, MoO_3 (h-MoO_3) is one of the promising nanofillers among the various metal oxides or metals due to its good chemical stability, excellent wear resistance, high hardness, and eco-friendliness [13,14]. So far, no studies have reported the preparation of h-MoOx composites for corrosion-resistant coatings.

Furthermore, the increasing demand for low carbon coating is attracting more attention due to the discharging of volatile organic compounds (VOCs) during the conventional solvent coating process. Hence, here we developed the coating composites at room temperature without any solvent addition. In this work, a simple coating prepared by incorporating MoO_3 into the WEP matrix was coated on the steel surface. Firstly, MoO_3 nanorods were optimized and obtained via a modified precipitation method. Subsequently, composite WEP coatings were prepared with the addition of low content of MoO_3 (0.5%). With the

synthesized MoO_3 nanofiller, our work aims to investigate the enhanced anticorrosion properties of the new MoO_3/WEP composites.

2. Materials and Methods

2.1. Materials

The materials ammonium molybdate tetrahydrate ($H_{24}Mo_7N_6O_{24}\cdot 4H_2O$), high-tempe rature resistant dimethyl silicone oil, sodium chloride (NaCl), and potassium chloride (KCl) were purchased from Aladdin Industrial Corporation. All reagents were analytical grade without further purification. Epoxy resin and curing agent were purchased from Zanxi Resin Co., Ltd (Shanghai, China).

2.2. Synthesis of MoO_3 Composite Coating

MoO_3 nanoparticles were synthesized using a modified precipitation method [15]. Briefly, 10.0 g of ammonium molybdate was slowly added to a round-bottom flask with 100 g deionized water. The solution was magnetically stirred at room temperature for 2.5 h using a ceramic magnetic stirrer (Ronhua HJ-3, Changzhou, China), and then 2 M of HNO_3 solution was added continuously until the pH of the mixture reached 1 ± 0.1. The above mixture was further heated at 90 ± 1 °C in a silica oil-bath for 12 h. After that, the white precipitations (Figure 1a) were filtered with 0.45 µm PTFE filter membrane and washed with deionized water and ethanol several times. The obtained product was dried in the vacuum condition at 60 °C for 12 h, and the product was collected for the subsequent characterization and analysis. To obtain the optimal MoO_3 rods with the desired particle size and morphology, pH (1, 1.5, 2, and 2.5), reaction temperature (80 and 90 °C), and stirring rate (250, 350, and 450 rpm) were adjusted during the synthesis process.

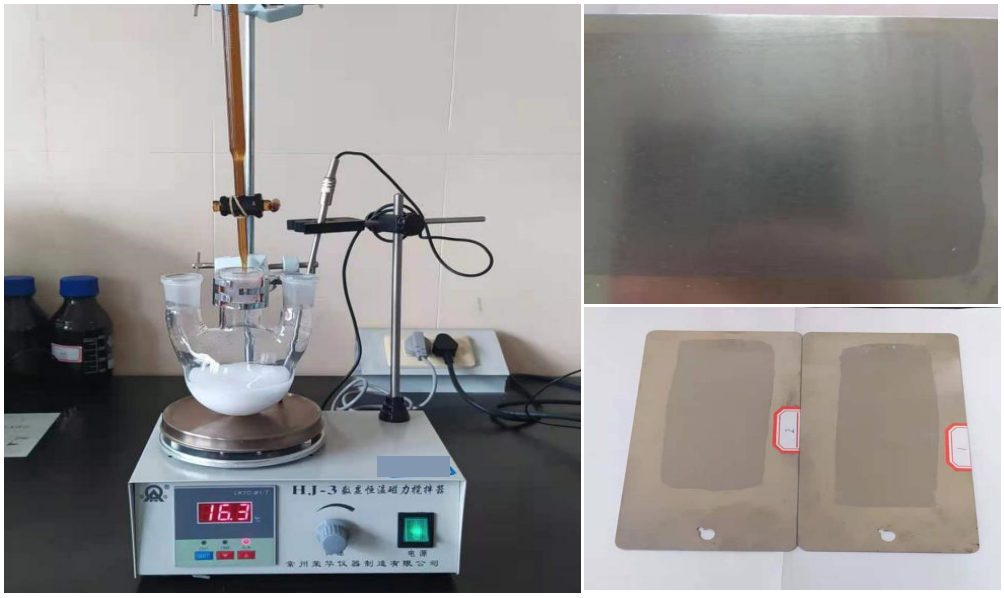

(**a**) (**b**)

Figure 1. Laboratory set-up: (**a**) MoO_3 synthesis set-up and (**b**) MoO_3/WEP coating sample.

For the preparation of anticorrosion coating, the WEP resin was first obtained by mixing the epoxy resin, deionized water, and the curing agent. Then, the 0.5 wt.% of MoO_3 was added to the epoxy matrix to obtain the homogeneous mixture. The nanocomposite mixture was then coated on the polished steel panel (Q-lab, Westlake, OH, US) via a film applicator (bar coater) to control the coating film thickness (Figure 1b). The wet film thickness was about 100 µm. The dry film thickness was 35 µm, tested by a thickness gauge (BEVS1703, Shenhua Industrial Co. Ltd., Shanghai, China).

2.3. Characterization of MoO_3

X-ray diffraction (XRD) measurements were conducted with Cu Ka radiation (36 kV, 20 mA) in an XD-6 X-ray diffractometer (Purkinje General Instrument Co., Ltd. Beijing, China). The morphology of MoO_3 nanoparticles was analyzed using a field emission scanning electron microscope (FESEM, Hitachi S-4800, Japan), which operated in secondary electron yield mode and with a beam energy of 10 keV.

2.4. Electrochemistry Anticorrosion Testing of MoO_3/WEP Coating

The anticorrosion experiments were performed in a CHI660D Electrochemistry Workstation (Chenhua Instrument Co., Ltd., Shanghai, China). The setup was equipped with three electrodes, namely the coating sample as the working electrode, saturated calomel electrode as the reference one, and platinum slide as the counter electrode. EIS testing was carried out at open circuit potential with the frequency range of 100 kHz to 0.01 Hz. The potential fluctuation was not beyond 5 mV prior to the test. For all the measurements, the EIS spectra were repeated to ensure the data is reliable.

3. Results and Discussion

3.1. Optimization of MoO_3 Synthesis: SEM Morphology

Figure 2 shows the morphologies of the synthesized MoO_3. Generally, our SEM results indicated that the optimal conditions for the synthesis of MoO_3 nanorods were pH = 1, 90 °C reaction temperature, and medium stirring rate (350 rpm). It is worth noting that pH significantly influenced the morphology of MoO_3. Specifically, when pH was 2.5, SEM results showed that the microstructure corresponded to isostructural belts with a diameter of >1 μm (Figure 2c). When pH was reduced to 1, the particle diameter was shortened to around 200 nm (Figure 2b). For the MoO_3 synthesized with different stirring rates, the best morphology was achieved only under the medium rate (350 rpm), as characterized by SEM. This result is consistent with the crystal nucleation theory during the precipitation [16]. The synthesis operating at a high mixing rate (>350 rpm) could result in a very high nucleation rate, and the inhomogeneous particle morphologies were observed accordingly. A very high crystal growth rate could be obtained at the low mixing rate (<350 rpm); thus, the desired particle size and the ideal morphologies could not be achieved in this case.

3.2. Optimization of MoO_3 Synthesis: XRD Characterization

The XRD patterns of MoO_3 were further investigated under the different conditions of pH, stirring rate and reaction temperature. As shown in Figure 3, the optimized MoO_3 spectrum (pH = 1, T = 90 °C, stirring rate = 350 rpm) presented the reflection angles located at 2θ = 9.69, 16.74, 19.45, 25.80, 29.35, 35.45, and 45.47°. These sharp peaks corresponded to (100), (110), (200), (210), (300), (310), and (410) crystal planes of h-MoO_3, which are consistent with the standard spectrum (JCPDF:21-0569), and these peaks were in accordance with the previously reported hexagonal crystal h-MoO_3 [17]. The results also suggested that the sample was MoO_3 nanorod, with no other impurities. Interestingly, higher pH (pH > 2) could lead to the different crystalline phase structures (Figure 4). The spectra presented the different reflection angles located at 2θ = 13.95, 23.09, 26.95, 28.08, 29.73, 47.21, and 53.37°, which corresponded to (200), (020), (311), (202), (211), (040), and (513) crystal planes of MoO_3 and identified the sample as orthorhombic crystal α-MoO_3 according to the standard spectrum (JCPDF 46-1048). Our result was consistent with a previous study showing that H^+ concentration was crucial for MoO_3 grain growth and crystal structure [18]. The as-prepared α-MoO_3 was a microscale belt with a diameter of ~1 μm (Figure 2c, Section 2.1). The microscale particle size is too large to be incorporated into this coating for a film thickness of 35 μm, so α-MoO_3 was not employed for the subsequent coating studies. The XRD spectra of samples synthesized under other reaction conditions (temperature and mixing rate) are not presented here due to them having relatively more impurity peaks or lower intensity.

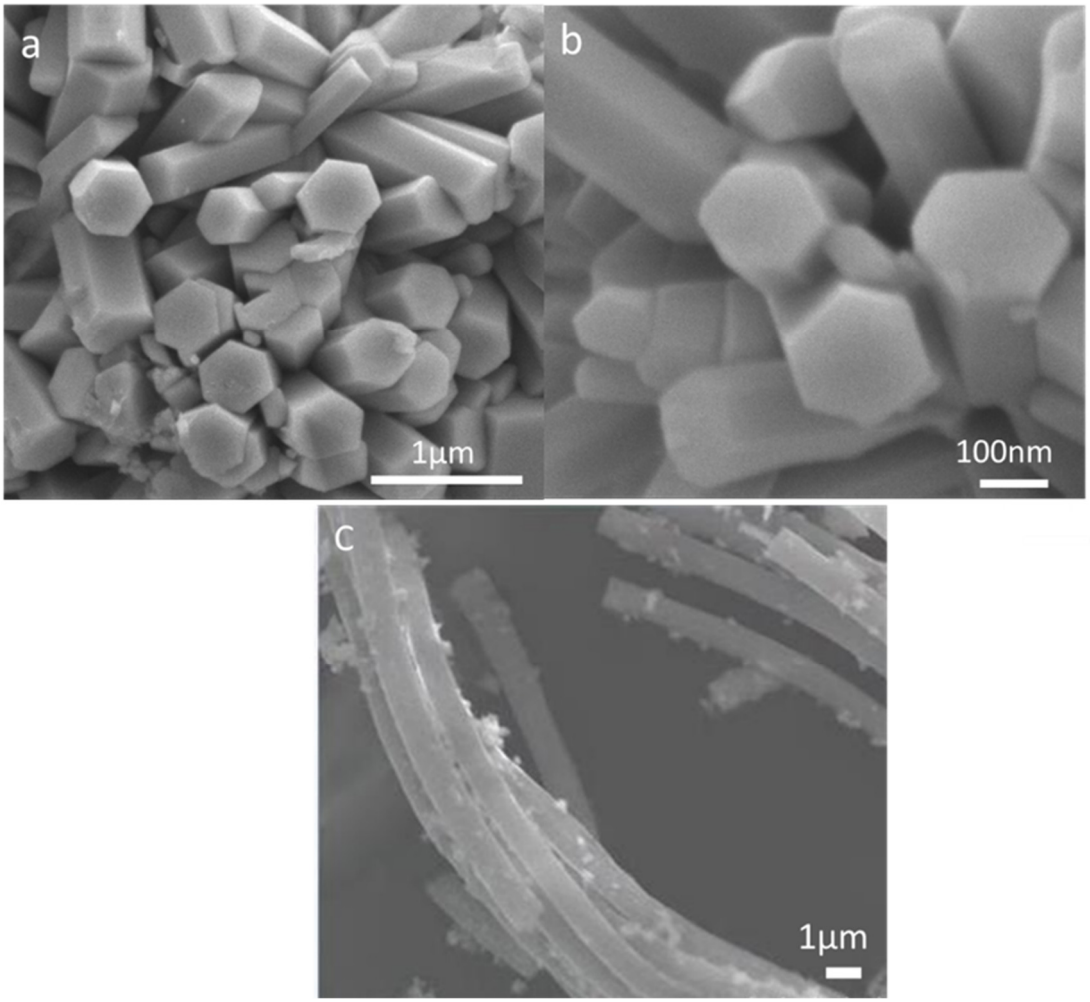

Figure 2. SEM images of optimally synthesized MoO_3 with magnifications of (**a**) ×30,000 and (**b**) ×70,000 (optimal synthesis conditions: pH = 1, reaction temperature: 90 °C, medium stirring rate: 350 rpm). (**c**) SEM images of synthesized MoO_3 with magnification of ×7500 (synthesis conditions: reaction temperature: pH = 2.5, T = 90 °C, medium stirring rate: 350 rpm).

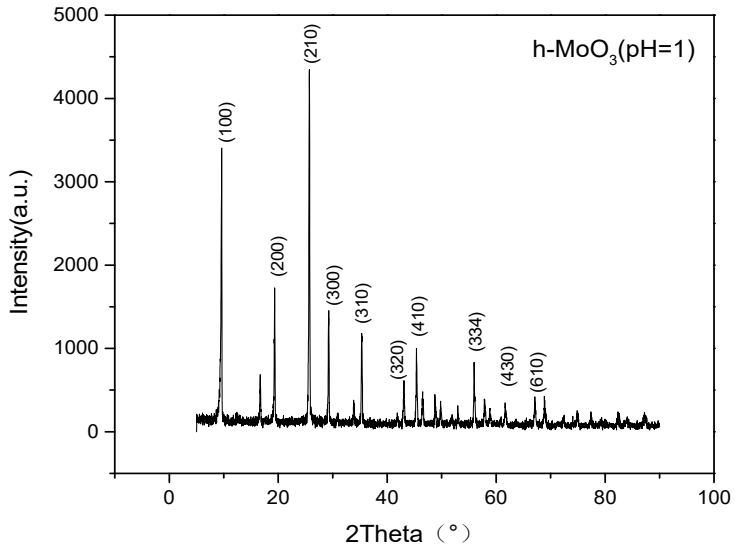

Figure 3. XRD pattern of h-MoO_3 under the optimized synthesis conditions: pH = 1, T = 90 °C, medium stirring rate (350 rpm).

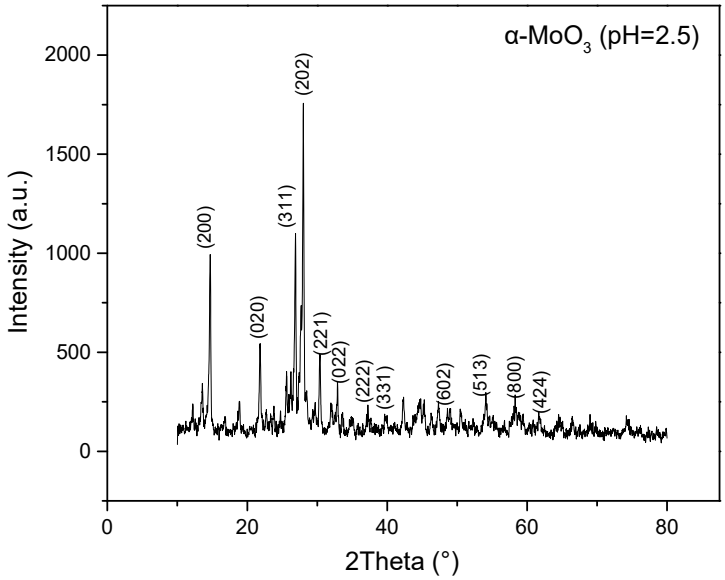

Figure 4. XRD pattern of α-MoO_3 under the synthesis conditions pH = 2.5, T = 90 °C, medium stirring rate (350 rpm).

3.3. Electrochemical Impedance Spectroscopy (EIS) Testing

In this experiment, electrochemical corrosion properties were evaluated according to the composite coating. Figure 5 presents the Bode plots of WEP only and MoO_3/WEP containing 0.5 wt.% h-MoO_3 nanocomposite coatings on steel in 3.5 wt.% NaCl solution. Based on the Bode plots, the magnitude of the impedance in the low-frequency zone (0.01 Hz) can be applied to evaluate the corrosion resistance performance [19,20]. For the control WEP coating, the Bode impedance remained at a constant value initially and then decreased after immersion on the 30th day (Figure 5d). That of the MoO_3/WEP sample was almost constant for up to 30 days. The results indicated that the polarization resistance increased with the addition of h-MoO_3 nanoparticles in the epoxy matrix during the testing period. For both short-term (1 day, Figure 5a) and long-term (30 days, Figure 5d) immersion, the MoO_3/WEP composite coatings had a relatively higher impedance modulus at low-frequency zone (0.01 Hz), which suggested that the composites could promote the corrosion protection of epoxy coating by incorporating h-MoO_3 nanofillers. This was mainly attributed to the nanorods extending the permeation of moisture and ions into the coatings, which is consistent with previous reports [11,12].

Our results showed that with 30 days of immersion, the MoO_3/WEP composite coating could maintain stable anticorrosion enhancement. Therefore, the nanocomposite has a beneficial effect on the anticorrosion performance of the tested materials. Our results clearly show that the h-MoO_3 nanorods can be a promising candidate nanofiller for epoxy or similar polymeric coatings compared with the coatings without nanoparticle addition.

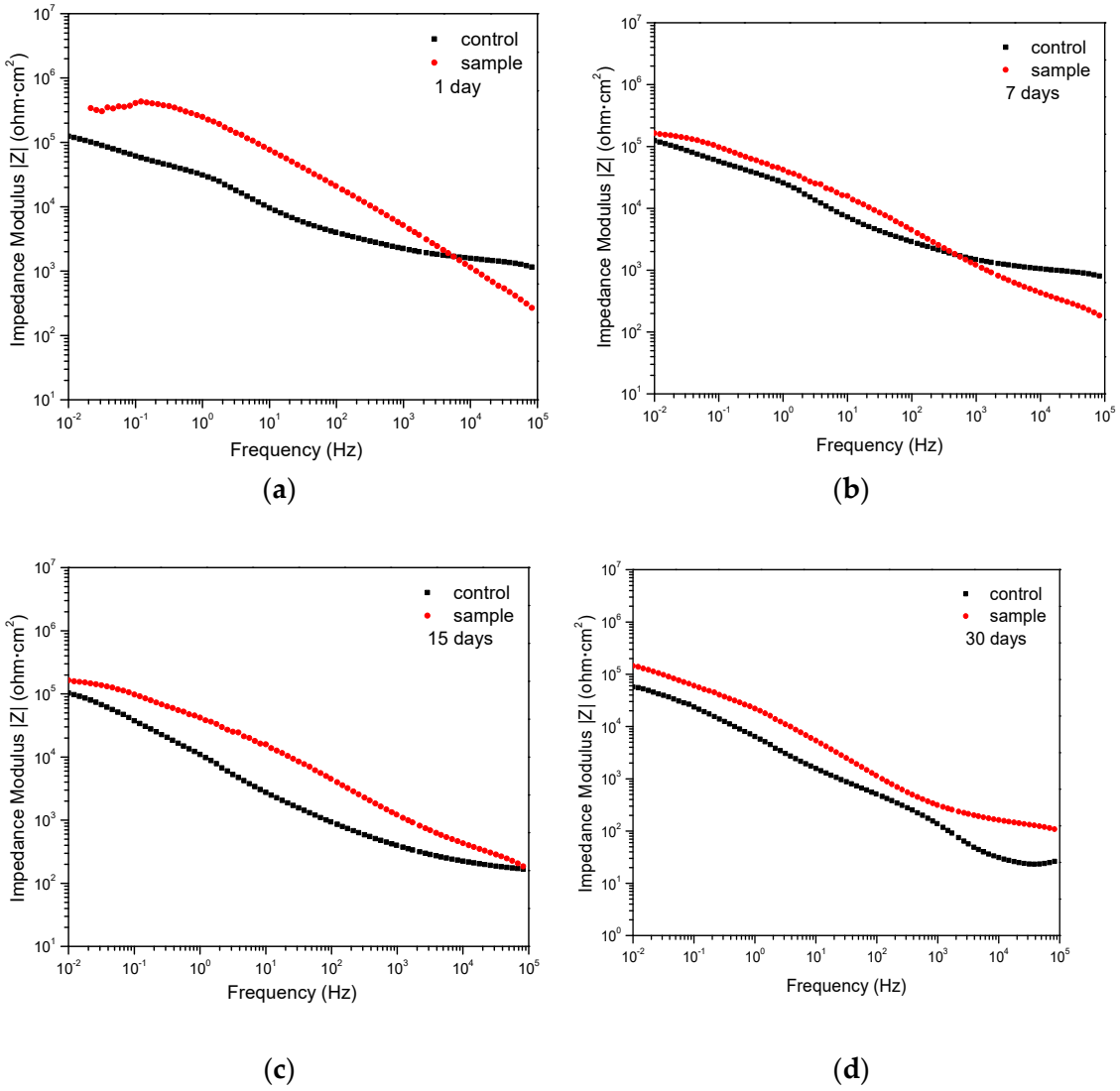

Figure 5. EIS spectrum of the optimally synthesized MoO_3. (**a**) The composite coating sample immersed in 3.5% NaCl solution for 1 day; (**b**) the sample immersed in 3.5% NaCl solution for 7 days; (**c**) the sample immersed in 3.5% NaCl solution for 15 days and (**d**) 30 days.

4. Conclusions

In this study, a novel approach was developed by incorporating 1D h-MoO_3 nanofillers into a WEP matrix to promote the corrosion resistance of the composite coatings. The MoO_3 nanoparticles were first synthesized based on the modified precipitation method. The h-MoO_3 nanorod synthesis parameters were optimized as pH = 1, T = 90 °C, and stirring rate = 350 rpm based on XRD and SEM investigation. Subsequently, the anticorrosive performance of the MoO_3/WEP coating was evaluated by EIS studies in 3.5 wt.% NaCl solution. The anticorrosion performance of the composite coating was improved significantly by the incorporation of 0.5 wt.% MoO_3 nanorods. Therefore, h-MoO_3 nanorods have the potential to be further applied to commercially available coatings to improve corrosion resistance.

Author Contributions: Project administration, supervision, conceptualization, methodology, writing, formal analysis, Y.Z. and Q.Z.; investigation, formal analysis, data curation, draft preparation, C.S. and Z.C. All authors have read and agreed to the published version of the manuscript.

Funding: This research received no external funding.

Acknowledgments: We gratefully acknowledge the financial support of faculty funding from Huzhou University (China).

Conflicts of Interest: The authors declare no conflict of interest.

References

1. Hays, G.F. World Corrosion Organization, Corrodia, Fall. 2010. Available online: http://events.nace.org/euro/corrodia/Fall_2010/wco.asp (accessed on 28 January 2016).
2. Wu, X.; Zheng, S. Transparent Icephobic Coatings Using Bio-Based Epoxy Resin. *Mater. Des.* **2018**, *140*, 516–523. [CrossRef]
3. Singh, P.K.; Modanwal, R.P. Fabrication and Mechanical Characterization of Glass Fiber/Al_2O_3 Hybrid-Epoxy Composite. *Sādhanā* **2021**, *46*, 1–10. [CrossRef]
4. Sviridova, T.V.; Logvinovich, A.S. Electrochemical Growing of Ni-MoO_3 Nanocomposite Coatings Via Redox Mechanism. *Surf. Coat. Technol.* **2017**, *319*, 6–11. [CrossRef]
5. Slawinski, W.A.; Fjellvag, O.S. A Novel Polytype—the Stacking Fault Based Gamma-MoO_3 Nanobelts. *Acta Crystallogr B Struct. Sci. Cryst. Eng. Mater.* **2016**, *72*, 201–208. [CrossRef] [PubMed]
6. Zaman, I.; Phan, T.T.; Kuan, H.-C.; Meng, Q.; La, L.T.B.; Luong, L.; Youssf, O.; Ma, J. Epoxy/graphene platelets nanocomposites with two levels of interfacestrength. *Polymer* **2011**, *52*, 1603–1611. [CrossRef]
7. Zhang, Q.; Xu, Y.; Wen, Z. Influence of water-borne epoxy resin content on performance of waterborne epoxy resin compound SBR modified emulsified asphalt for tack coat. *Constr. Build. Mater.* **2017**, *153*, 774–782. [CrossRef]
8. Moghaddam, A.R.; Ranjbar, Z.; Sundararaj, U.; Jannesari, A.; Kamkar, M. A novel electrically conductive water borne epoxy nanocomposite coating based on graphene: Facile method and high efficient graphene dispersion. *Prog. Org. Coat.* **2019**, *136*, 105223. [CrossRef]
9. Fang, Y.; Wang, P.; Sun, L.; Wang, L. The Effect of Graphene Nanofiller on the Surface Structure and Performance of Epoxy Resin-Polyhedral Oligomeric Silsesquioxane (Ep-Poss). *Nanomaterials* **2021**, *11*, 841. [CrossRef] [PubMed]
10. Shukla, M.K.; Sharma, K. Effect of Carbon Nanofillers on the Mechanical and Interfacial Properties of Epoxy Based Nanocomposites: A Review. *Polym. Sci.* **2019**, *61*, 439–460.
11. Fihri, A.; Abdullatif, D. Decorated Fibrous Silica Epoxy Coating Exhibiting Anti-Corrosion Properties. *Prog. Org. Coat.* **2019**, *127*, 110–116. [CrossRef]
12. Liu, H.; Wang, X. Durable Molybdenum Oxide Coated Solid-Phase Microextraction Fiber for Highly Selective and Efficient Extraction of Polycyclic Aromatic Hydrocarbons in Water. *J. Sep. Sci.* **2019**, *42*, 1878–1885. [CrossRef] [PubMed]
13. Wang, Z.; Madhavi, S.; Lou, X.W. Ultralong α-MoO3 Nanobelts: Synthesis and Effect of Binder Choice on Their Lithium Storage Properties. *J. Phys. Chem. C* **2012**, *116*, 12508–12513. [CrossRef]
14. Vipin, K.; Xu, W. Formation of hexagonal-molybdenum trioxide (h-MoO_3) nanostructures and their pseudocapacitive behavior. *Nanoscale* **2015**, *21*, 11777–11786.
15. Hang, N.N.; Enrico, T.N.; Bryan, G.A.; Debora, F.R. Designing polymeric adhesives for antimicrobial materials: Poly(ethylene imine) polymer, graphene, graphene oxide and molybdenum trioxide-a biomimetic approach. *J. Mater. Chem. B* **2017**, *28*, 6616–6628.
16. Rajaeiyan, A.; Bagheri-Mohagheghi, M.M. Comparison of sol-gel and co-precipitation methods on the structural properties and phase transformation of γ and α-Al_2O_3 nanoparticles. *Adv. Manuf.* **2013**, *1*, 176–182. [CrossRef]
17. Kumar, S.; Singh, A.; Singh, R.; Singh, S.; Kumar, P.; Kumar, R. Facile h-MoO3 synthesis for NH_3 gas sensing application at moderate operating temperature. *Sens. Actuators B Chem.* **2020**, *325*, 1–21. [CrossRef]
18. Jittiarporn, P.; Sikong, L.; Kooptarnond, K.; Taweepreda, W.; Chooto, P.; Khangkhamano, M. Synthesis of h-MoO_3 and (NH4)2Mo4O13 using precipitation method at various pH values and their photochromic properties. *App. Mecha. Mater.* **2016**, *835*, 34–41. [CrossRef]
19. Hinderliter, B.R.; Croll, S.G.; Tallman, D.E.; Su, Q.; Bierwagen, G.P. Interpretation of EIS data from accelerated exposure of coated metals based on modeling of coating physical properties. *Electrochim. Acta* **2006**, *51*, 4505–4515. [CrossRef]
20. Sarkar, N.; Sahoo, G.; Das, R.; Prusty, G.; Sahu, D.; Swain, S. Anticorrosion performance of three-dimensional hierarchical PANI@BN nanohybrids. *Ind. Eng. Chem. Res.* **2016**, *55*, 2921–2931. [CrossRef]